Stem Cell Reports
Report
ISSCR
OPEN ACCESS

Derivation of Brain Capillary-like Endothelial Cells from Human Pluripotent Stem Cell-Derived Endothelial Progenitor Cells

Catarina Praça,[1,2,4] Susana C. Rosa,[2] Emmanuel Sevin,[3] Romeo Cecchelli,[3] Marie-Pierre Dehouck,[3] and Lino S. Ferreira[2,4,*]
[1]Doctoral Programme in Experimental Biology and Biomedicine (PDBEB), Portugal CNC - Center for Neuroscience and Cell Biology, University of Coimbra, Coimbra, Portugal
[2]Center for Neuroscience and Cell Biology, University of Coimbra, Coimbra, Portugal
[3]Faculté des Sciences Jean Perrin, Université d'Artois, Lens, France
[4]Faculty of Medicine, University of Coimbra, Coimbra, Portugal
*Correspondence: lino@uc-biotech.pt
https://doi.org/10.1016/j.stemcr.2019.08.002

SUMMARY

The derivation of human brain capillary endothelial cells is of utmost importance for drug discovery programs focusing on diseases of the central nervous system. Here, we describe a two-step differentiation protocol to derive brain capillary-like endothelial cells from human pluripotent stem cells. The cells were initially differentiated into endothelial progenitor cells followed by specification into a brain capillary-like endothelial cell phenotype using a protocol that combined the induction, in a time-dependent manner, of VEGF, Wnt3a, and retinoic acid signaling pathways and the use of fibronectin as the extracellular matrix. The brain capillary-like endothelial cells displayed a permeability to lucifer yellow of 1×10^{-3} cm/min, a transendothelial electrical resistance value of 60 Ω cm^2 and were able to generate a continuous monolayer of cells expressing ZO-1 and CLAUDIN-5 but moderate expression of P-glycoprotein. Further maturation of these cells required coculture with pericytes. The study presented here opens a new approach for the study of soluble and non-soluble factors in the specification of endothelial progenitor cells into brain capillary-like endothelial cells.

INTRODUCTION

The blood-brain barrier (BBB) is a physical and metabolic barrier formed by a specialized network of brain capillary endothelial cells (BCECs) that together with pericytes, astrocytes, microglia, neurons, and extracellular matrix (ECM) form the functional neurovascular unit (NVU). BCECs are characterized by their low permeability to drugs, mostly due to the high expression of tight junctions as well as the molecular influx and efflux transporters that selectively regulate the flux of molecules through the BBB (Abbott et al., 2010; Aday et al., 2016; Cecchelli et al., 2007; Zhao et al., 2015). In addition, BCECs present low vesicle trafficking, resulting in low rates of transcytosis (Siegenthaler et al., 2013; Villaseñor et al., 2018).

Pluripotent stem cells are a promising source of cells for the derivation of large numbers of brain capillary-like endothelial cells (BCLECs) to study BBB function in homeostasis and disease such as Alzheimer and Parkinson diseases. Up until now, BCLECs have been derived from induced pluripotent stem cells (iPSCs) based on differentiation protocols relying on non-defined media (i.e., containing serum) (Appelt-Menzel et al., 2017; Katt et al., 2016, 2018; Lim et al., 2017; Lippmann et al., 2012, 2014; Ribecco-Lutkiewicz et al., 2018) or chemically defined media (Hollmann et al., 2017) without the isolation of endothelial progenitor cells (EPCs). In these protocols, BCLECs have been selectively purified from a mixture of different cell populations containing neural progenitor cells by using selective media and ECM. Unfortunately, the heterogeneity inherent to the system precludes the study of the molecular mechanisms governing the specification of iPSCs into BCLECs. Furthermore, the yield and the final phenotype of the BCLECs obtained was dependent on the original iPSC line used (Lippmann et al., 2012). During the preparation of this work, a protocol for the derivation of BCLECs using an intermediary EPC population and chemically defined media was reported (Qian et al., 2017). The protocol consisted of the differentiation of iPSCs into EPCs (characterized by the expression of VEGFR2 and CD31) followed by their specification into BCLECs by exposure to retinoic acid (RA). Yet, the role of other soluble and non-soluble signaling molecules on BCLEC specification, the cell kinetics during specification, as well as the permeability properties of BCLEC monolayers to small molecules, were not investigated.

Here, we describe a method to derive BCLECs from iPSCs based on the initial differentiation of iPSCs into EPCs followed by their specification into BCLECs by modulating three different signaling pathways (VEGF, RA, and WNT) and providing variable ECM substrates. We monitored the process by following the expression of BCEC markers by flow cytometry, immunocytochemistry, and gene expression analyses. To assess the functional properties of the BCLECs obtained, we evaluated the transendothelial electrical resistance (TEER), paracellular permeability, response to pro-inflammatory stimuli, and transport of P-glycoprotein (PGP) ligands. The BCLECs reported here

This is an open access article under the CC BY-NC-ND license (http://creativecommons.org/licenses/by-nc-nd/4.0/).

are immature in nature but open new opportunities for future BBB disease modeling and drug-screening initiatives.

RESULTS

Characterization of EPCs

iPSCs were differentiated for 10 days in conditions that promoted mesoderm differentiation (Figure 1A). Then, EPCs were isolated by magnetic activated cell sorting (MACS), and the expression of BEC markers was performed by flow cytometry (Figure 1B) and immunocytochemistry (Figure 1C). Approximately 91% of the sorted cells expressed CD31, 90% VEGFR2, 97% GLUT-1, 51% CLAUDIN-5, 58% OCCLUDIN, and the expression of PGP was not detected (Figure 1B). The EPCs obtained were able to uptake acetylated low-density lipoprotein (ac-LDL) and expressed OCCLUDIN, CLAUDIN-5, and ZO-1 without colocalization with cell junctions, suggesting that these cells were not yet specified into BCLECs (Figure 1C).

Screening of Soluble Factors for the Specification of EPCs into BCLECs

VEGF (Engelhardt and Liebner, 2014), WNT (Daneman et al., 2009; Liebner et al., 2008; Stenman et al., 2008; Zhou and Nathans, 2014; Wang et al., 2018), and RA (Lippmann et al., 2014; Qian et al., 2017; Mizee et al., 2013) signaling have been reported as important players in early phases of BBB development. To specify EPCs into BCLECs, we modulated the three above-mentioned signaling pathways in a temporal manner (Figure 2A) using concentrations (VEGF, 50 ng/mL, Ferreira et al., 2007; Wnt3a, 10 ng/mL, Cecchelli et al., 2014; RA, 10 μM, Lippmann et al., 2014) previously reported by us and others. Importantly, EPCs (passage 1) expressed frizzled receptors (*FZD4*, *FZD6*, and *FZD7*) (Figure S1A1) and the concentration of Wnt3a used was enough to increase mRNA transcripts of downstream players of the Wnt3a signaling pathway, namely *LEF1* and *APCDD1* (Liebner et al., 2008; Lippmann et al., 2012) (Figure S1A2). No significant differences were observed for *AXIN2*. EPCs were cultured for four passages onto fibronectin-coated dishes in basal medium (BM) supplemented, or not, with different factors, and the expression of BCEC markers was monitored over time by flow cytometry and qRT-PCR. The selection of fibronectin was based on the fact that, during the early stages of angiogenesis, when the specification of endothelial cells (ECs) into BCECs starts, ECs express predominantly fibronectin receptors (α4β1 and α5β1 integrins) (Milner and Campbell, 2002; Wang and Milner, 2006). Since collagen IV and fibronectin proteins are both part of the NVU ECM, we also tested the use of a combined mix of these substrates, but no improvement was seen (data not shown). The expression of EC markers was lower in cells cultured in BM or BM + Wnt3a (Figures 2B and 2C) than in the remaining conditions, suggesting that these culture conditions were less efficient in maintaining the EC phenotype. Because non-ECs have a significant impact on the barrier properties of ECs (Figure S1B), $CD31^+$ cells were purified and cultured to confluency on Matrigel-coated Transwell inserts for 6 days after which paracellular permeability to lucifer yellow (LY) and TEER analyses were performed. The monolayer of purified cells cultured in BM showed a relatively high permeability to LY ($3 \pm 0.6 \times 10^{-3}$ cm/min) (Figure 2D) and low TEER (ca. $22.3 \pm 1.5\ \Omega\ cm^2$) (Figure 2E). The supplementation of BM with individual factors reduced the permeability of the EC barrier to LY (VEGF, $1.8 \pm 0.3\times10^{-3}$ cm/min; Wnt3a, $1.6 \pm 0.1\times10^{-3}$ cm/min; RA, $2.4 \pm 0.3\times10^{-3}$ cm/min) (Figure 2D). Interestingly, the supplementation of BM with a combination of factors (protocol 5, BM supplemented with VEGF and Wnt3a; protocol 6, BM supplemented with VEGF, Wnt3a, and RA) yielded an EC barrier with higher TEER values (BM + VEGF + Wnt3a, $50 \pm 0.8\ \Omega\ cm^2$; BM + VEGF + Wnt3a + RA, $55 \pm 0.6\ \Omega\ cm^2$) (Figure 2E) and lower paracellular permeability to LY (BM + VEGF + Wnt3a, $1.2 \pm 0.2 \times 10^{-3}$ cm/min; BM + VEGF + Wnt3a + RA, $1.2 \pm 0.1 \times 10^{-3}$ cm/min) than cells cultured with BM or BM supplemented with each factor alone (Figure 2D). Thus, our results showed that BM supplemented with VEGF, Wnt3a, and RA offered the best approach to differentiate EPCs into BCLECs and generate a monolayer of cells with the highest TEER values and lowest paracellular permeability to LY. This chemically defined medium was selected for the remaining experiments.

Screening of ECM for the Specification of EPCs into BCLECs

ECM is an important component for the maintenance of BBB integrity (Baeten and Akassoglou, 2011; del Zoppo and Milner, 2006). To evaluate the role of ECM in the induction of a BCEC phenotype from EPCs, we obtained decellularized ECM from primary bovine pericytes, bovine brain capillary endothelial cells (bBCECs), and rat glial cells (Figure S2). We found that the best time to decellularize the cell monolayers was between day 8 and day 12, based on a compromise between the amount of deposited ECM and time (data not shown). In these conditions, regardless of the cell type, we obtained a decellularized matrix consisting of 1.5–2 $\mu g/cm^2$ of collagen (Figure S2C), which is in line with the value described for decellularized matrix obtained from mesenchymal stem cells (Prewitz et al., 2013). In addition, the decellularized matrix had relatively low levels of sulfated glycosaminoglycan (sGAG) (0.11 $\mu g/cm^2$ for bBCECs; data not shown), again in accordance with other studies (Prewitz et al., 2013). To evaluate the stability of the decellularized ECM, the matrices were kept in culture

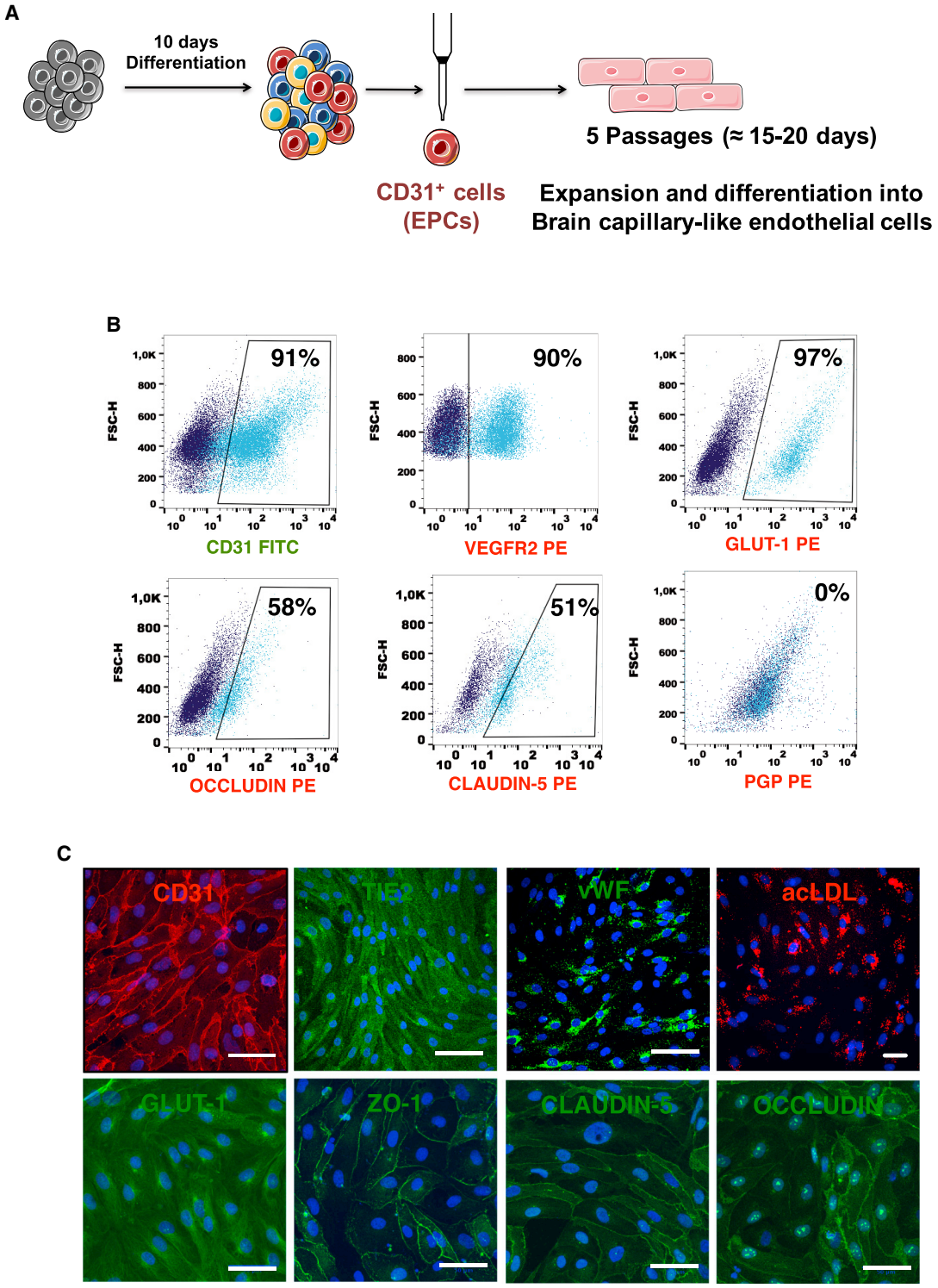

Figure 1. Characterization of EPCs

(A) Scheme of iPSCs differentiation into BCLECs. iPSCs were first differentiated during 10 days into EPCs ($CD31^+$ cells). These cells were then isolated by MACS and specified/expanded into BCLECs for four passages.

(B) Expression of BCEC markers was assessed by flow cytometry on isolated $CD31^+$ cells. Percentages of positive cells were calculated based on the isotype controls (1%; dark blue scatter plot).

(C) Expression of BCEC markers on $CD31^+$ cells by immunocytochemistry. Scale bar corresponds to 50 μm.

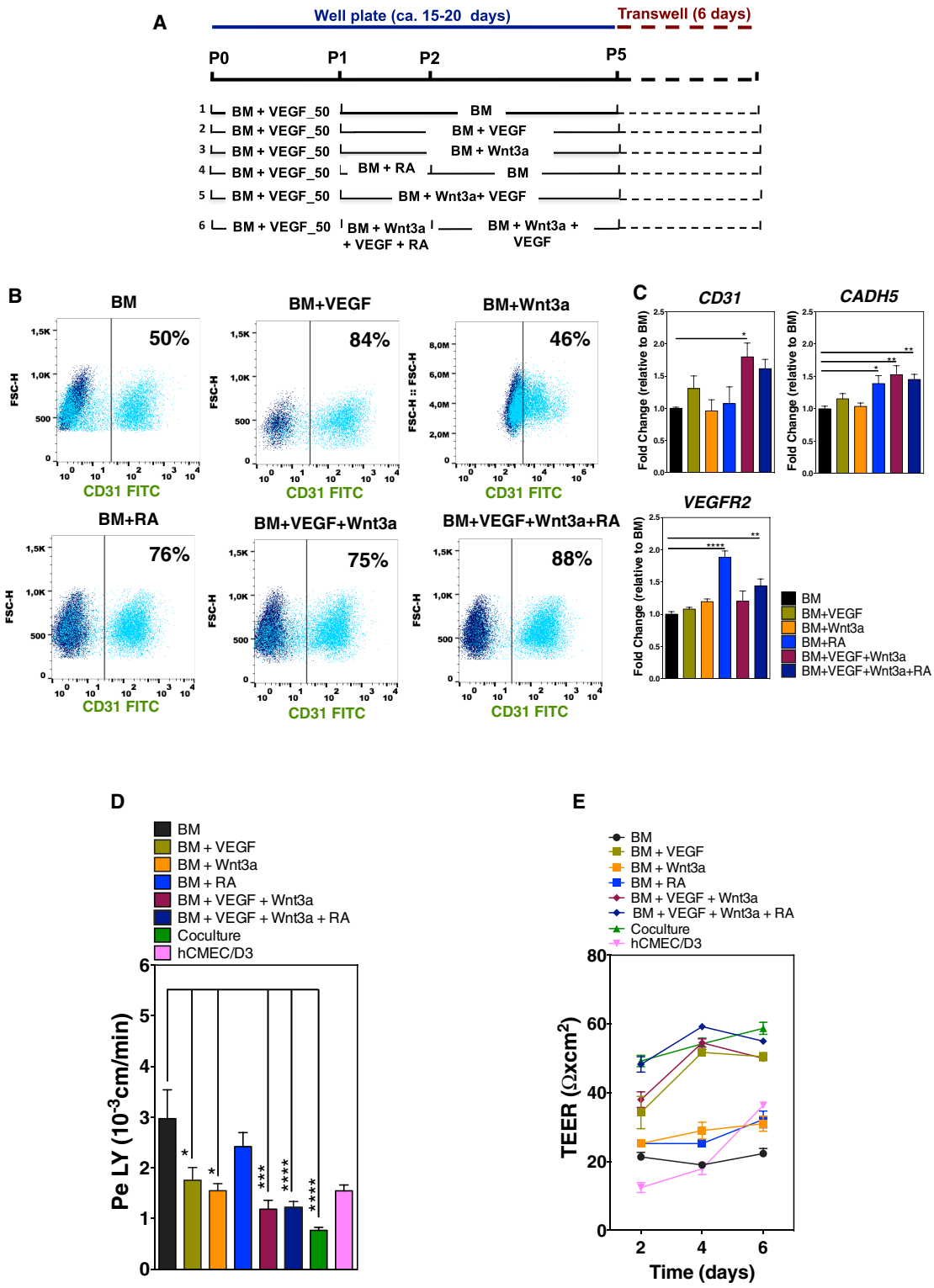

Figure 2. Effect of Soluble Factors on the Specification of EPCs into BCLECs

(A) Schematic representation of the protocols used to specify CD31$^+$ onto BCLECs.

(B) Expression of CD31 marker on ECs at passage 4 was assessed by flow cytometry. Percentages of positive cells were calculated based on the isotype controls (1%; dark blue scatter plot).

(legend continued on next page)

medium, 4°C or 37°C, for 4 days, and our results showed that approximately 50% of the collagen content was maintained after 4 days, regardless of the temperature (Figure S2D). Taken together, our results showed that we could prepare decellularized ECM from cells of the NVU.

To evaluate the effect of decellularized ECM in the induction of BCEC phenotype from EPCs, CD31$^+$ cells were cultured on top of decellularized ECMs or fibronectin (control) for three passages (ca. 12 days), both in BM or BM supplemented with VEGF, Wnt3a, and RA (Figure 3A). CD31$^+$ cells adhered to glial and bBCEC decellularized ECM; however, they did not adhere well to the decellularized ECM of pericytes and died after some time. Therefore, only cells cultured on fibronectin and decellularized glial or bBCEC ECMs were characterized by flow cytometry at passage 4. Cells cultured in the glial decellularized ECM presented a lower co-expression of CD31:ZO-1 and CD31:CLAUDIN-5 and a higher co-expression of CD31:PGP than the ones cultured on fibronectin (Figure S2E1). Colocalization results, combined with the expression of BCEC markers (Figure S2E), suggested that cells cultured on glial decellularized ECM expressed BBB markers, but they were not all CD31$^+$ cells. Cells cultured on decellularized bBCEC ECM significantly lost their endothelial phenotype (as evaluated by CD31 marker) and showed low co-expression of CD31:ZO-1, CD31:CLAUDIN-5, and CD31:PGP (Figure S2E). These studies were complemented by gene analyses for a set of ECM, ECs, and BCEC genes (Table S1) (Armulik et al., 2010; Cecchelli et al., 2014; Lippmann et al., 2012). Gene clustering analyses showed that CD31$^+$ cells cultured on fibronectin and BM supplemented with VEGF, Wnt3a, and RA were more related to BCECs derived from a coculture of ECs (differentiated from human hematopoietic progenitor cells) with pericytes, previously described by us (coculture condition; Cecchelli et al., 2014) (Figure 3B). Similar results were obtained using high-throughput gene expression analyses by Fluidigm (Figure S2F). Therefore, the decellularized glial ECM did not significantly improve the BCEC phenotype compared with fibronectin.

Next, we evaluated the functional properties of the BCLECs obtained at passage 5 after purification using the CD31 marker. BCLECs were cultured to confluence on Transwell inserts for 6 days after which paracellular permeability to LY and TEER analyses were performed. Cells cultured onto the decellularized glial ECM and fibronectin, but not in bBCEC ECM, expressed VE-CADHERIN, CLAUDIN-5, and ZO-1 at the cell borders and showed intercellular communication (Figure 3C). No difference in paracellular permeability to LY was observed between cells cultured onto fibronectin or onto decellularized ECM from glial cells; however, cells cultured onto decellularized bBCEC ECM showed higher paracellular permeability than cells cultured in the other conditions (Figure 3D). On the other hand, cells cultured onto fibronectin had higher TEER values than the ones cultured in the other conditions (Figure 3E).

Overall, our results showed that from the three decellularized ECMs tested, only decellularized glial ECM showed promising results in terms of EC phenotype maintenance, induction of BCEC markers, and paracellular permeability; however, the results were not significantly different from the ones obtained with fibronectin. Therefore, subsequent tests were performed with CD31$^+$ cells cultured on fibronectin-coated plates in BM supplemented with VEGF, Wnt3a, and RA.

Specification of EPCs into BCLECs: Effect of Time and Pluripotent Stem Cell Line

The induction of BCLEC properties in CD31$^+$ cells cultured on fibronectin-coated plates in the presence of BM supplemented with VEGF, Wnt3a, and RA was monitored by flow cytometry and compared with CD31$^+$ cells cultured in BM alone. Flow cytometry analyses were performed at passage 2 (approximately 8 days in culture) and 4 (approximately 16 days in culture), and the colocalization of the CD31 marker with ZO-1, CLAUDIN-5, or PGP was quantified. Our results showed that cells cultured in BM supplemented with VEGF, Wnt3a, and RA have higher colocalization of CD31 with ZO-1 or CLAUDIN-5 (Figure 4A), and this was further confirmed by confocal microscopy analyses (Figure S3A). As expected, the expression of BCEC markers was higher than the one observed in initial EPCs (Figures 1B and 1C) or ECs without a BBB phenotype (Figure S3B) and similar, for some markers, to BCECs (hCMEC/D3 cell

(C) Fold change of endothelial gene expression in ECs cultured in the different protocols at passage 4 (without purification) relative to ECs cultured in BM conditions. Genes were normalized against the control gene *ACTB*. Values are means ± SEM (n = 3 independent experiment, 3 technical replicates per experimental condition). *$p < 0.05$, **$p < 0.01$, and ****$p < 0.0001$ using one-way ANOVA followed by Dunnett's multiple comparison test.

(D and E) (D) Paracellular permeability to LY and (E) TEER in cells either exposed or not to the chemical factors with purification 6 days after being plated on Matrigel-coated Transwell inserts. In (D) and (E), the hCMEC/D3 cell line and human hematopoietic progenitor cell-derived ECs cocultured with pericytes for 6 days (coculture condition) (Cecchelli et al., 2014) were used as controls. Values are means ± SEM (n = 3 independent experiments; at least 3 Transwell inserts per independent experiment and experimental condition). *$p < 0.05$, ***$p < 0.001$, and ****$p < 0.0001$ using one-way ANOVA followed by Dunnett's multiple comparison test.

See also Figure S1.

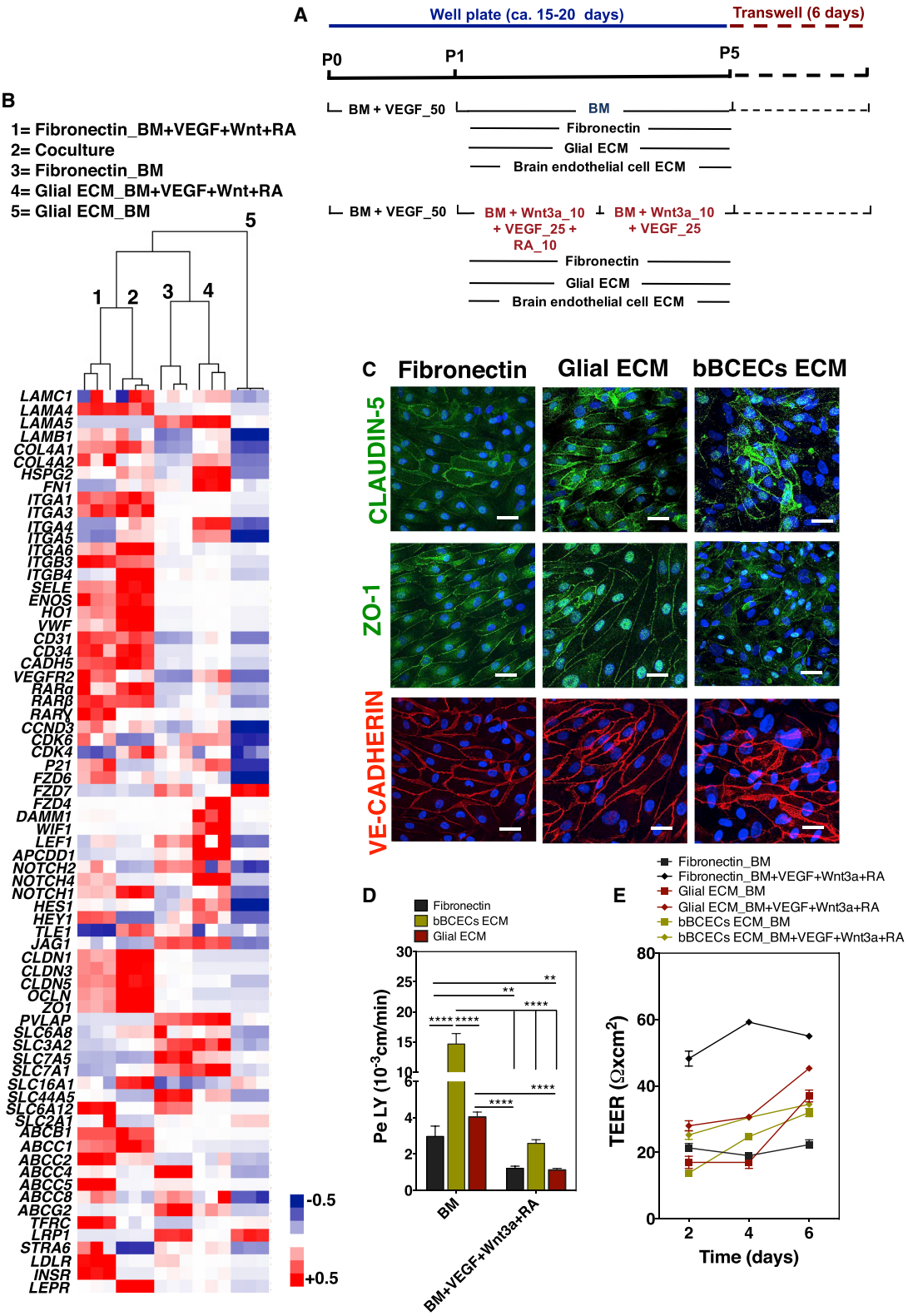

(legend on next page)

line) (Figure S3C). Noteworthy, the colocalization between CD31 and ZO-1/CLAUDIN-5 increased over time even though the differentiated cells expressed very low levels of PGP. Interestingly, our results showed that the CD31$^-$ subpopulation also expressed BCEC markers, likely indicating the presence of intermediate phenotypic stages in the cell population (Figure 4A).

We next tested whether our differentiation protocol could generate BCLECs using different human pluripotent stem cell lines, including the human embryonic stem cell line NKX2-5$^{eGFP/W}$ (Elliott et al., 2011) and the iPSC cell line derived from a Hutchinson-Gilford progeria syndrome (HGPS) fibroblast (Nissan et al., 2012). Using both pluripotent cell lines, we were able to reproduce the differentiation protocol, ultimately obtaining BCLECs expressing endothelial and BCEC markers (Figures S3D and S3E).

Functional Characterization of BCLECs

CD31$^+$ cells were cultured on fibronectin-coated plates in the presence of BM supplemented with VEGF, Wnt3a, and RA for four passages. At passage 5, cells were again purified for CD31 marker and grown to confluence on Transwell inserts for 6 days, after which the monolayer was characterized by immunocytochemistry (Figure 4B). Cells expressed typical endothelial surface markers, such as CD31, VE-CADHERIN, and TIE-2, as well as intracellular markers such as von WILLEBRAND FACTOR (vWF), and were able to uptake ac-LDL (Figure 4B). Moreover, the cells obtained expressed BCEC markers, including the tight-junction proteins ZO-1, CLAUDIN-5, OCCLUDIN, and GLUT-1 (Figure 4B). The transporter PGP was expressed at moderate levels (Figure 4B). Furthermore, at transcriptional level, the differentiated cells showed lower expression of plasmalemma vesicle-associated protein (*PVLAP*) and a higher expression of multiple BBB genes such as tight junctions (*CLDN1* and *ZO1*), influx amino acid (*SLC16A1*), receptors (e.g., insulin receptor [*INSR*], transferrin receptor [*TFRC*] and low-density lipoprotein receptor-related protein [*LRP1*]) and key efflux transporters such as *ABCB1* and multidrug resistance protein (*ABCC1* and *ABCC5*) than cells differentiated in BM conditions (Figure 4C). Based on the gene and protein expression results, as well as the paracellular permeability and TEER results (Figures 2C and 2D), the differentiated cells were named as BCLECs.

BCLECs constitutively expressed intracellular adhesion molecule (ICAM)-1 and -2 and responded to inflammatory stimuli such as tumor necrosis factor alpha (TNF-α) (Figure 4D). ICAM-1 was upregulated in BCLECs (Figure 4D) and HUVECs (control; Figure S4A) exposed to TNF-α, likely mediated by the activation of the pleiotropic nuclear factor kB (NF-kB) (Collins et al., 1995), while ICAM-2 was slightly downregulated in BCLECs after TNF-α, according to what is observed in HUVECs (Figure S4A) and previous studies (McLaughlin et al., 1998), compared with the basal expression. BCLECs had no measurable expression of VCAM-1 by flow cytometry (data not shown), in agreement with other studies (Halaidych et al., 2018).

Because the expression of PGP in BCLECs was moderate, we evaluated whether the coculture with other cells from NVU would affect its expression and activity. We assessed the PGP activity and expression in BCLECs, with or without coculture for 6 days with bovine pericytes. The expression of PGP was not statistically different in BCLECs cocultured with pericytes compared with BCLECs cultured as a monoculture (Figure 4E). Our results further showed that the inhibition of the PGP by elacridar led to a significant increase in the accumulation of Rhodamine 123 in BCLECs cocultured with pericytes but not when they were absent (Figure 4F).

Overall, the BCLECs obtained using our protocol expressed BCEC markers at gene and protein levels, they responded to inflammatory stimuli such as TNF-α, and they

Figure 3. Effect of the Combination of Soluble Factors with Decellularized ECMs in the Specification of EPCs into BCLECs

(A) Schematic representation of the protocols used to maturate the CD31$^+$ to BCLECs. Cells were cultured for three passages either on fibronectin (control) or on decellularized ECM and then purified and plated on Matrigel-coated Transwell inserts for 6 days.

(B) Relative gene expression levels on cells cultured on BM or BM + VEGF + Wnt3a + RA either on fibronectin or glial ECM (positive control was "coculture" condition, i.e., human hematopoietic stem/progenitor-derived ECs cocultured with pericytes; Cecchelli et al., 2014) followed by plating on Matrigel-coated Transwell inserts for 6 days. The heatmap and hierarchical clustering dendogram are displayed. Genes were normalized against the control gene *ACTB* (n = 1 independent experiment, 3 technical replicates per experimental condition). Relative gene expression is provided in Table S1. For each gene, the normalized values were between +0.5 and −0.5 (see Supplemental Information for the detailed calculation procedure). Gene expression that was above the gene expression median for all the experimental groups is shown in red, the expression below the median in blue, and the expression similar to the median in white.

(C) Expression of CLAUDIN-5, ZO-1, and VE-CADHERIN in BCLECs plated on Matrigel-coated Transwell inserts for 6 days. Scale bar corresponds to 50 μm.

(D and E) (D) Paracellular permeability to LY and (E) TEER on cells specified in different ECMs and media followed by their purification and culture for 6 days on Matrigel-coated Transwell inserts. In (D) and (E), values are means ± SEM (n = 3 independent experiments; at least 3 Transwell inserts per independent experiment and experimental condition). $^{**}p < 0.01$ and $^{****}p < 0.0001$ using one-way ANOVA followed by Tukey's multiple comparison test.

See also Figure S2.

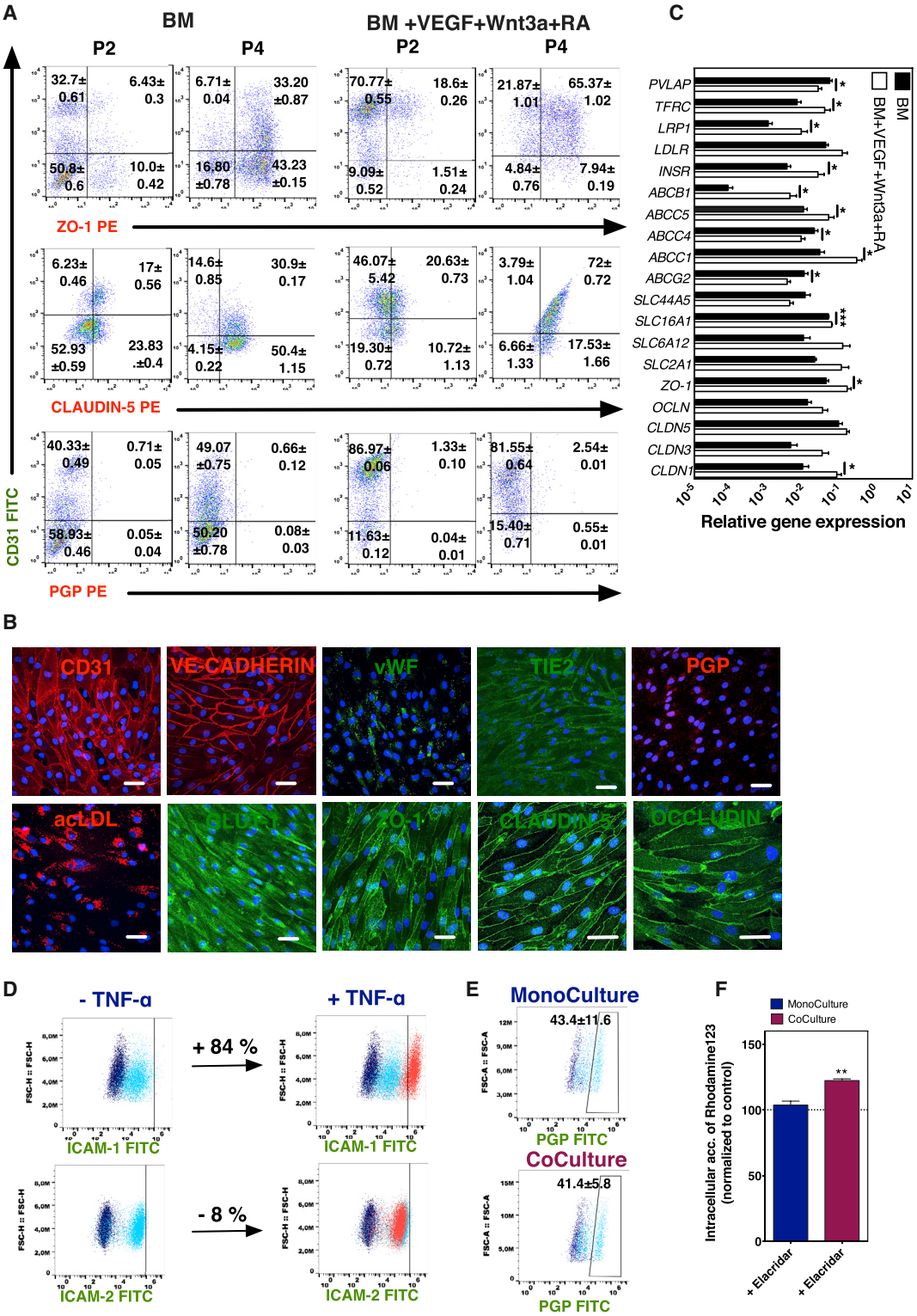

Figure 4. Impact of Time on the Specification of EPCs into BCLECs and BCLEC Functional Characterization

(A) Expression by flow cytometry of BCEC markers (ZO-1, CLAUDIN-5, and PGP) colocalized with CD31 marker on cells specified in different inductive media (BM and BM + VEGF + Wnt3a + RA) at passage 2 and passage 4. Percentages of positive cells were calculated based on the isotype controls (1%).

(legend continued on next page)

showed efflux transporter activity when further maturated in coculture with pericytes.

DISCUSSION

In this study, we described the derivation of BCLECs from iPSCs using a two-step protocol. Initially, we derived EPCs from human iPSCs, after which they were specified into a BCLEC phenotype by exposure to both soluble and insoluble cues. After screening several soluble and insoluble factors, we showed that EPCs cultured on fibronectin for four passages (ca. 15–20 days) in BM supplemented with Wnt3a, VEGF, and RA had a high expression of endothelial markers (CD31, VE-CADHERIN, vWF), organized tight junctions at cell-cell junctions (ZO-1, CLAUDIN-5, OCCLUDIN), expressed nutrient transporters (GLUT-1) and some of them (ca. 40% of the cells) expressed efflux pumps (PGP), had a TEER similar to other human BCECs (TEER of ca. 60 Ω cm^2) (Cecchelli et al., 2014), displayed a paracellular permeability of 1×10^{-3} cm/min to LY and, upon exposure to TNF-α, they upregulated adhesion molecules such as ICAM-1 and downregulated ICAM-2. Overall, the ECs obtained showed a BCLEC phenotype. The current approach to generate BCLECs under fully chemically defined medium and ECM is desirable since (1) it will be more reproducible than existing protocols based on the use of KnockOut serum replacement or Matrigel-based substrates and (2) it can contribute to unravel the mechanism(s) governing the specification into BCLEC. Indeed, here we show that the addition of Wnt3a at later stages improved the barrier properties of the cells in monolayer (Figure S4B), while the use of a coculture with pericytes in the presence of soluble factors identified in the current study did not improve the barrier properties (Figure S4C). Moreover, the current approach recapitulates the developmental stages of rodent embryonic BBB formation, i.e., formation of EPCs that respond to VEGF signaling, followed by the specification of these cells into BCECs by the modulation of WNT signaling among other signaling pathways (Engelhardt and Liebner, 2014). Further studies are necessary to investigate whether this developmental recapitulation is extensive to human BBB development.

Recent studies have shown the derivation of BCLECs from iPSCs using a heterogeneous population of cells during differentiation and in non-defined media (Appelt-Menzel et al., 2017; Katt et al., 2016, 2018; Lim et al., 2017; Lippmann et al., 2012, 2014; Ribecco-Lutkiewicz et al., 2018). The differentiation protocol yielded on average 11.6 BCLECs per input iPSC, characterized by the co-expression of CD31 and GLUT-1 markers. These cells co-expressed CLAUDIN-5 (~100%), OCCLUDIN (~100%), GLUT-1 (~70%), and PGP (~70%) (Lippmann et al., 2012, 2014). Our differentiation protocol yielded on average 10 BCLECs per input iPSC and the cells obtained co-expressed CLAUDIN-5 (~90%), OCCLUDIN (~100%), GLUT-1 (~100%), and PGP (~40%). Although the focus of the current work was to investigate the involvement of soluble and non-soluble factors, as well as the dynamics, in the generation of a BCLEC phenotype from EPCs, much more effort is warranted to create a mature and functional BBB model characterized by cell polarization (not investigated in the current work), a high TEER, and PGP expression as observed in primary BCECs (Hartmann et al., 2007) and other iPSC-derived BBB models (Qian et al., 2017). One of the major differences between our model and the ones previously described is related to the TEER values. It is important to note that TEER measurements are influenced by several parameters, including the equipment, temperature, medium composition and the area of the well, thus comparison of TEER values between models and laboratories is difficult (Deli et al., 2005; Srinivasan et al., 2015). Although the *in vivo* TEER is estimated to be between 1,000 and 2,000 Ω cm^2 in rat or frog brains (Butt et al., 1990; Crone and Olesen, 1982), the *in vivo* TEER in humans remains to be determined. Moreover, the high TEER observed by some iPSC-derived BCLECs (Lippmann et al., 2012; Qian et al.,

(B) Expression of BCEC markers on BCLECs by immunofluorescence after 6 days on Matrigel-coated Transwell inserts. Scale bar corresponds to 50 μm.

(C) Relative gene expression on cells plated on Matrigel-coated Transwell inserts for 6 days after specification on BM or BM + VEGF + Wnt3a + RA. Genes were normalized against the control gene *ACTB*. Values are means ± SEM (n = 3 independent experiment, 3 technical replicates per experimental condition). *$p < 0.05$ and ***$p < 0.001$ using unpaired t test.

(D) Expression of adhesion molecules (ICAM-1 and ICAM-2) on BCLECs at basal level and after exposure to TNF-α (10 ng/mL) for 24 hr. Percentage of positive cells was calculated based in the gates defined for the basal expression of the marker (1%; light blue scatter plot).

(E) Expression of PGP on BCLECs cultured alone or in coculture with pericytes for 6 days on Matrigel-coated Transwell inserts. The percentage of positive cells was calculated based on the gates defined for the isotype control (1%; dark blue scatter plot). Values are means ± SEM (n = 3 independent experiments). No statistical difference was observed between means as evaluated by an unpaired t test.

(F) Accumulation of Rhodamine 123 after inhibition of BCLECs cultured alone or in coculture with pericytes for 6 days on Matrigel-coated Transwell inserts with elacridar. Values are means ± SEM (n = 3 independent experiments; 3 Transwell inserts per independent experiment and experimental condition). **$p < 0.01$ using unpaired t test.

See also Figures S3 and S4.

2017) has been questioned recently by single-cell RNA analyses, which have demonstrated that the cells presenting high TEER might have a neuroectodermal epithelial cell phenotype and not a BCLEC phenotype (Lu et al., 2019). Future studies should investigate the effect of the initial density of EPCs in the functional outcome of BCLECs, as this variable might play an important role in differentiation/maturation of BCLECs (Qian et al., 2017; Wilson et al., 2015). In addition, to achieve a physiological barrier model, the effect of decellularized matrices from NVU at the end of the specification process as well as the use of cocultures with cells from NVU should be investigated. Indeed, our results indicate that the coculture of BCLECs with pericytes further mature the cells as confirmed by a higher activity of PGP and low expression of transcripts of transcytosis genes (*PVLAP* and *CAV1*) (Ben-Zvi et al., 2014; Daneman et al., 2010) (Figure S4D) compared with a monoculture of BCLECs.

The control of Wnt3a, VEGF, and RA signaling pathways seems important for the specification of EPCs into BCLECs. Previous studies using iPSCs have shown that canonical Wnt-β-catenin (Lippmann et al., 2012) and RA (Katt et al., 2016; Lippmann et al., 2014) signaling was necessary for the specification of BBB properties in ECs. Our results further showed that the use of VEGF was important to maintain the endothelial phenotype during the specification of the cells.

ECM provides physical support and presents biomolecules that may be important for the BBB specification process (Daneman et al., 2010; Katt et al., 2016). Previous studies have demonstrated that ECM produced by cells forming the NVU (glial and pericytes) improved the barrier function of BCECs cultured *in vitro* (Hartmann et al., 2007). Others have evaluated the effect of artificial ECMs such as Matrigel in the differentiation of iPSCs into BCECs (Patel and Alahmad, 2016). The current study evaluates the effect of decellularized ECM from the NVU in the specification of iPSCs into BCLECs. Our results showed that EPCs were unable to adhere to pericyte decellularized ECM, but they could attach to the decellularized matrix of bBCECs and glial cells. Cells differentiated on top of decellularized glial ECM showed the highest BCLEC phenotype after four passages, the highest TEER, and the lowest paracellular permeability to LY. However, the results obtained were not significantly different from the ones obtained on fibronectin-coated dishes. We cannot discard the possibility that the decellularized ECM might play a role in the polarization of BCLECs, a topic that deserves further investigation in the near future. Moreover, the decellularized matrices from NVU were obtained from animal sources (bovine pericytes, bBCECs, and rat glial cells) due to availability reasons. Future studies should explore the impact of decellularized ECMs of human origin.

The work presented here may contribute to a better understanding of the processes underlying BBB development and maintenance. BBB formation is initiated at embryonic day 12 in the rat cerebral cortex by ECs that invade the neural tissue from the surrounding vascular plexus (Daneman et al., 2010). BBB-forming ECs are characterized by the expression of tight junctions, including OCCLUDIN, CLAUDIN-5 and ZO-1, and the influx transporter GLUT-1. Interestingly, these cells express low levels of PGP that only increase during postnatal development (Daneman et al., 2010). Our *in vitro* results recapitulate this process since moderate levels of PGP were observed in BCLECs. Previous studies have derived BCLECs with high expression of PGP, which may indicate a high level of maturation (Katt et al., 2016; Lippmann et al., 2012). In addition, our results showed that the specification of EPCs into BCLECs is a slow process given that the expression of ZO-1, CLAUDIN-5, and PGP increased in $CD31^+$ cells over four passages. Because $CD31^-$ cells also expressed BCEC markers, future studies should further characterize these cells as well as their importance in the formation of a BBB.

Overall, the methodology reported in this work opens an opportunity to study the effect of soluble and non-soluble factors in the specification of EPCs into BCLECs, the dynamics of BCEC markers expression, and the functionality of the derived cells.

EXPERIMENTAL PROCEDURES

Details are provided in Supplemental Experimental Procedures.

Derivation of BCLECs

iPSCs cell lines generated from human cord blood (passages, 30–40; K2-iPSC line) (Haase et al., 2009) or from HGPS fibroblasts (passages, 43–51) (Nissan et al., 2012) were used in the present study and were provided by the laboratories in which they were derived. For some experiments, the human embryonic stem cell line NKX2-5$^{eGFP/W}$ (passages, 40–45) (Elliott et al., 2011) was used. To initiate the differentiation, iPSCs (27×10^3–45×10^3 cells per cm^2) were treated for 45–60 min with collagenase IV and plated on fibronectin-coated dishes (1 μg/cm^2; Calbiochem) in a chemically defined medium (CDM) (see Supplemental Information). During the 10 days of the differentiation, several factors were added to CDM in order to induce the formation of EPCs ($CD31^+$ cells) (Rosa et al., 2019). $CD31^+$ cells were isolated by MACS (Miltenyi Biotec), plated on fibronectin-coated dishes (1 μg/cm^2), and cultured in EGM-2 (Lonza) supplemented with SB 431542 (10 μM; Tocris Biosciences), basic fibroblast growth factor (bFGF; 1 ng/mL; Sigma), and $VEGF_{165}$ (50 ng/mL; PeproTech) for one passage. Cells were then cultured in BM (EGM-2 supplemented with 10 μM SB 431542 and 1 ng/mL bFGF) or BM supplemented with $VEGF_{165}$ (25 ng/mL), Wnt3a (10 ng/mL; R&D Systems), or RA (10 μM; Sigma), alone or in combination, for three passages

(approximately 15–20 days; Figure 2A). In a separate set of experiments, $CD31^+$ cells were plated on fibronectin-coated dishes or in decellularized native ECMs from pericytes, glial cells, and bBCECs in the presence of BM or BM supplemented with $VEGF_{165}$, Wnt3a, and RA (Figure 3A). During the differentiation procedure, cells were passed systematically every 4 days, in a split ratio of 1:3. Cells plated in the Transwell inserts were cultured in EGM-2 supplemented with bFGF (1 ng/mL).

Statistical Analyses

For analyses involving three or more groups, an ANOVA test was used followed by Dunnett's or Tukey's post test. For analysis of two groups, an unpaired t test was used. Statistical analysis was performed using GraphPad Prism software. Results were considered significant when $p \leq 0.05$. In the case of results with three independent runs and three technical replicates per independent run, the statistics were performed based on the nine values (not by the means of each experiment).

SUPPLEMENTAL INFORMATION

Supplemental Information can be found online at https://doi.org/10.1016/j.stemcr.2019.08.002.

AUTHOR CONTRIBUTIONS

L.S.F., C.P., and S.C.R. conceived the study. C.P. and S.C.R. performed cell culture and decellularization experiments, gene, flow cytometry, immunocytochemistry, LY and TEER analyses. E.S., R.C., and M.-P.D. performed PGP inhibition studies and contributed with neural cells. All authors contributed to manuscript preparation.

ACKNOWLEDGMENTS

L.S.F. is grateful for funding from the Portugal2020 project StrokeTherapy (ref. 3386), EC project ERA chair (ERA@UC, ref. 669088) and FCT projects (PTDC/DTP-FTO/2784/2014 and 02/SAICT/2017/029229). C.P. and S.C.R. would like to thank the FCT for fellowships (SFRH/BD/51678/2011; SFRH/BPD/79323/2011, respectively).

Received: July 22, 2018
Revised: August 5, 2019
Accepted: August 6, 2019
Published: September 5, 2019

REFERENCES

Abbott, N.J., Patabendige, A.A., Dolman, D.E., Yusof, S.R., and Begley, D.J. (2010). Structure and function of the blood-brain barrier. Neurobiol. Dis. *1*, 13–25.

Aday, S., Cecchelli, R., Hallier-Vanuxeem, D., Dehouck, M.P., and Ferreira, L. (2016). Stem cell-based human blood-brain barrier models for drug discovery and delivery. Trends Biotechnol. *5*, 382–393.

Appelt-Menzel, A., Cubukova, A., Gunther, K., Edenhofer, F., Piontek, J., Krause, G., Stuber, T., Walles, H., Neuhaus, W., and Metzger, M. (2017). Establishment of a human blood-brain barrier co-culture model mimicking the neurovascular unit using induced pluri- and multipotent stem cells. Stem Cell Reports *4*, 894–906.

Armulik, A., Genove, G., Mae, M., Nisancioglu, M.H., Wallgard, E., Niaudet, C., He, L., Norlin, J., Lindblom, P., Strittmatter, K., et al. (2010). Pericytes regulate the blood-brain barrier. Nature *7323*, 557–561.

Baeten, K.M., and Akassoglou, K. (2011). Extracellular matrix and matrix receptors in blood-brain barrier formation and stroke. Dev. Neurobiol. *11*, 1018–1039.

Ben-Zvi, A., Lacoste, B., Kur, E., Andreone, B.J., Mayshar, Y., Yan, H., and Gu, C. (2014). Mfsd2a is critical for the formation and function of the blood-brain barrier. Nature *7501*, 507–511.

Butt, A.M., Jones, H.C., and Abbott, N.J. (1990). Electrical resistance across the blood-brain barrier in anaesthetized rats: a developmental study. J. Physiol. *429*, 47–62.

Cecchelli, R., Berezowski, V., Lundquist, S., Culot, M., Renftel, M., Dehouck, M.P., and Fenart, L. (2007). Modelling of the blood-brain barrier in drug discovery and development. Nat. Rev. Drug Discov. *8*, 650–661.

Cecchelli, R., Aday, S., Sevin, E., Almeida, C., Culot, M., Dehouck, L., Coisne, C., Engelhardt, B., Dehouck, M.P., and Ferreira, L. (2014). A stable and reproducible human blood-brain barrier model derived from hematopoietic stem cells. PLoS One *6*, e99733.

Collins, T., Read, M.A., Neish, A.S., Whitley, M.Z., Thanos, D., and Maniatis, T. (1995). Transcriptional regulation of endothelial cell adhesion molecules: NF-kappa B and cytokine-inducible enhancers. FASEB J. *10*, 899–909.

Crone, C., and Olesen, S.P. (1982). Electrical resistance of brain microvascular endothelium. Brain Res. *1*, 49–55.

Daneman, R., Dritan Agalliu, D., Zhou, L., Kuhnert, F., Kuo, C.J., and Barres, B.A. (2009). Wnt/beta-catenin signaling is required for CNS, but not non-CNS, angiogenesis. Proc. Natl. Acad. Sci. U S A *106*, 641–646.

Daneman, R., Zhou, L., Kebede, A.A., and Barres, B.A. (2010). Pericytes are required for blood-brain barrier integrity during embryogenesis. Nature *7323*, 562–566.

Deli, M.A., Abraham, C.S., Kataoka, Y., and Niwa, M. (2005). Permeability studies on in vitro blood-brain barrier models: physiology, pathology, and pharmacology. Cell Mol. Neurobiol. *1*, 59–127.

Elliott, D.A., Braam, S.R., Koutsis, K., Ng, E.S., Jenny, R., Lagerqvist, E.L., Biben, C., Hatzistavrou, T., Hirst, C.E., Yu, Q.C., et al. (2011). NKX2-5(eGFP/w) hESCs for isolation of human cardiac progenitors and cardiomyocytes. Nat. Methods *12*, 1037–1040.

Engelhardt, B., and Liebner, S. (2014). Novel insights into the development and maintenance of the blood-brain barrier. Cell Tissue Res. *3*, 687–699.

Ferreira, L.S., Gerecht, S., Shieh, H.F., Watson, N., Rupnick, M.A., Dallabrida, S.M., Vunjak-Novakovic, G., and Langer, R. (2007). Vascular progenitor cells isolated from human embryonic stem cells give rise to endothelial and smooth muscle like cells and form vascular networks in vivo. Circ. Res. *3*, 286–294.

Haase, A., Olmer, R., Schwanke, K., Wunderlich, S., Merkert, S., Hess, C., Zweigerdt, R., Gruh, I., Meyer, J., Wagner, S., et al.

(2009). Generation of induced pluripotent stem cells from human cord blood. Cell Stem Cell *4*, 434–441.

Halaidych, O.V., Freund, C., van den Hil, F., Salvatori, D.C.F., Riminucci, M., Mummery, C.L., and Orlova, V.V. (2018). Inflammatory responses and barrier function of endothelial cells derived from human induced pluripotent stem cells. Stem Cell Reports *5*, 1642–1656.

Hartmann, C., Zozulya, A., Wegener, J., and Galla, H.-J. (2007). The impact of glia-derived extracellular matrices on the barrier function of cerebral endothelial cells: an in vitro study. Exp. Cell Res. *7*, 1318–1325.

Hollmann, E.K., Bailey, A.K., Potharazu, A.V., Neely, M.D., Bowman, A.B., and Lippmann, E.S. (2017). Accelerated differentiation of human induced pluripotent stem cells to blood-brain barrier endothelial cells. Fluids Barriers CNS *1*, 9.

Katt, M.E., Xu, Z.S., Gerecht, S., and Searson, P.C. (2016). Human brain microvascular endothelial cells derived from the BC1 iPS cell line exhibit a blood-brain barrier phenotype. PLoS One *4*, e0152105.

Katt, M.E., Linville, R.M., Mayo, L.N., Xu, Z.S., and Searson, P.C. (2018). Functional brain-specific microvessels from iPSC-derived human brain microvascular endothelial cells: the role of matrix composition on monolayer formation. Fluids Barriers CNS *1*, 7.

Liebner, S., Corada, M., Bangsow, T., Babbage, J., Taddei, A., Czupalla, C.J., Reis, M., Felici, A., Wolburg, H., Fruttiger, M., et al. (2008). Wnt/beta-catenin signaling controls development of the blood-brain barrier. J. Cell Biol. *3*, 409–417.

Lim, R.G., Quan, C., Reyes-Ortiz, A.M., Lutz, S.E., Kedaigle, A.J., Gipson, T.A., Wu, J., Vatine, G.D., Stocksdale, J., Casale, M.S., et al. (2017). Huntington's disease iPSC-derived brain microvascular endothelial cells reveal WNT-mediated angiogenic and blood-brain barrier deficits. Cell Rep. *7*, 1365–1377.

Lippmann, E.S., Azarin, S.M., Kay, J.E., Nessler, R.A., Wilson, H.K., Al-Ahmad, A., Palecek, S.P., and Shusta, E.V. (2012). Derivation of blood-brain barrier endothelial cells from human pluripotent stem cells. Nat. Biotechnol. *8*, 783–791.

Lippmann, E.S., Al-Ahmad, A., Azarin, S.M., Palecek, S.P., and Shusta, E.V. (2014). A retinoic acid-enhanced, multicellular human blood-brain barrier model derived from stem cell sources. Sci. Rep. *4*, 4160.

Lu, T.M., Redmond, D., Magdeldin, T., Nguyen, D.-H.T., Snead, A., Sproul, A., Xiang, J., Shido, K., Fine, H.A., Rosenwaks, Z., et al. (2019). Human induced pluripotent stem cell-derived neuroectodermal epithelial cells mistaken for blood-brain barrier-forming endothelial cells. bioRxiv https://doi.org/10.1101/699173.

McLaughlin, F., Hayes, B.P., Horgan, C.M., Beesley, J.E., Campbell, C.J., and Randi, A.M. (1998). Tumor necrosis factor (TNF)-alpha and interleukin (IL)-1beta down-regulate intercellular adhesion molecule (ICAM)-2 expression on the endothelium. Cell Adhes. Commun. *5*, 381–400.

Milner, R., and Campbell, I.L. (2002). Developmental regulation of beta1 integrins during angiogenesis in the central nervous system. Mol. Cell. Neurosci. *4*, 616–626.

Mizee, M.R., Wooldrik, D., Lakeman, K.A., van het Hof, B., Drexhage, J.A., Geerts, D., Bugiani, M., Aronica, E., Mebius, R.E., Prat, A., et al. (2013). Retinoic acid induces blood-brain barrier development. J. Neurosci. *4*, 1660–1671.

Nissan, X., Blondel, S., Navarro, C., Maury, Y., Denis, C., Girard, M., Martinat, C., De Sandre-Giovannoli, A., Levy, N., and Peschanski, M. (2012). Unique preservation of neural cells in Hutchinson- Gilford progeria syndrome is due to the expression of the neural-specific miR-9 microRNA. Cell Rep. *1*, 1–9.

Patel, R., and Alahmad, A.J. (2016). Growth-factor reduced Matrigel source influences stem cell derived brain microvascular endothelial cell barrier properties. Fluids Barriers CNS *13*, 6.

Prewitz, M.C., Seib, F.P., von Bonin, M., Friedrichs, J., Stissel, A., Niehage, C., Muller, K., Anastassiadis, K., Waskow, C., Hoflack, B., et al. (2013). Tightly anchored tissue-mimetic matrices as instructive stem cell microenvironments. Nat. Methods *8*, 788–794.

Qian, T., Maguire, S.E., Canfield, S.G., Bao, X., Olson, W.R., Shusta, E.V., and Palecek, S.P. (2017). Directed differentiation of human pluripotent stem cells to blood-brain barrier endothelial cells. Sci. Adv. *11*, e1701679.

Ribecco-Lutkiewicz, M., Sodja, C., Haukenfrers, J., Haqqani, A.S., Ly, D., Zachar, P., Baumann, E., Ball, M., Huang, J., Rukhlova, M., et al. (2018). A novel human induced pluripotent stem cell blood-brain barrier model: Applicability to study antibody-triggered receptor-mediated transcytosis. Sci. Rep. *1*, 1873.

Rosa, S., Praca, C., Pitrez, P.R., Gouveia, P.J., Aranguren, X.L., Ricotti, L., and Ferreira, L.S. (2019). Functional characterization of iPSC-derived arterial- and venous-like endothelial cells. Sci. Rep. *1*, 3826.

Siegenthaler, J.A., Sohet, F., and Daneman, R. (2013). 'Sealing off the CNS': cellular and molecular regulation of blood-brain barrier genesis. Curr. Opin. Neurobiol. *6*, 1057–1064.

Srinivasan, B., Kolli, A.R., Esch, M.B., Abaci, H.E., Shuler, M.L., and Hickman, J.J. (2015). TEER measurement techniques for in vitro barrier model systems. J. Lab. Autom. *2*, 107–126.

Stenman, J.M., Rajagopal, J., Carroll, T.J., Ishibashi, M., McMahon, J., and McMahon, A.P. (2008). Canonical Wnt signaling regulates organ-specific assembly and differentiation of CNS vasculature. Science *5905*, 1247–1250.

Villaseñor, R., Lampe, J., Schwaninger, M., and Collin, L. (2018). Intracellular transport and regulation of transcytosis across the blood–brain barrier. Cell Mol. Life Sci. *76*, 1081–1092.

Wang, J., and Milner, R. (2006). Fibronectin promotes brain capillary endothelial cell survival and proliferation through alpha5beta1 and alphavbeta3 integrins via MAP kinase signalling. J. Neurochem. *1*, 148–159.

Wang, Y., Cho, C., Williams, J., Smallwood, P.M., Zhang, C., Junge, H.J., and Nathans, J. (2018). Interplay of the Norrin and Wnt7a/Wnt7b signaling systems in blood–brain barrier and blood–retina barrier development and maintenance. Proc. Natl. Acad. Sci. U S A *50*, E11827–E11836.

Wilson, H.K., Canfield, S.G., Hjortness, M.K., Palecek, S.P., and Shusta, E.V. (2015). Exploring the effects of cell seeding

density on the differentiation of human pluripotent stem cells to brain microvascular endothelial cells. Fluids Barriers CNS *12*, 13.

Zhao, Z., Nelson, A.R., Betsholtz, C., and Zlokovic, B.V. (2015). Establishment and dysfunction of the blood-brain barrier. Cell *5*, 1064–1078.

Zhou, Y., and Nathans, J. (2014). Gpr124 controls CNS angiogenesis and blood-brain barrier integrity by promoting ligand-specific canonical wnt signaling. Dev. Cell *2*, 248–256.

del Zoppo, G.J., and Milner, R. (2006). Integrin-matrix interactions in the cerebral microvasculature. Arterioscler. Thromb. Vasc. Biol. *9*, 1966–1975.